

Manifestation of vibronic states in crystals of rare-earth compounds

V. A. Voloshin

Physicotechnical Institute, Academy of Sciences of the Ukrainian SSR, Donetsk

(Submitted 1 August 1985)

Zh. Eksp. Teor. Fiz. 90, 1336–1350 (April 1986)

Experimental data on the spectra of ethyl sulfates and molybdates are reported and analyzed on the basis of a hypothesis that a reduction in the distance between the central rare-earth ion and a ligand to $R < 2.38 \text{ \AA}$ makes the f electrons responsible for the chemical binding. Since the ground state of the rare-earth ion is degenerate or pseudodegenerate, the spectrum associated with the $4f$ configuration manifests a vibronic state, i.e., a state in which the nuclear and electron motions cannot be regarded separately. In this situation the experimental results demonstrate a strong reduction in the intensity of the lines due to "purely electronic" transitions in the absorption spectrum and those due to low-frequency vibrations in the Raman scattering spectrum. Thermal broadening and an increase in the distance in question above 2.38 \AA results in a situation when the chemical binding is again governed by the d electrons and the vibronic lines disappear from the spectrum associated with the $4f$ configuration.

A phase transition occurring in rare-earth ethyl sulfates under the influence of pressure was reported in 1979–80 (Refs. 1 and 2). Later³ a similar effect was revealed also by a spectroscopic study of $\text{CsDy}(\text{MoO}_4)_2$. We shall attempt to develop a model of microprocesses occurring as a result of phase transitions initiated by temperature and pressure in these two groups of substances.

1. APPARATUS

The main part of the present investigation was concerned with obtaining results at various pressures and temperatures. The only original feature was the apparatus used to generate high pressures. Figure 1 shows a high-pressure chamber used to record the Raman spectra. We can consider this chamber as representative of all the main features of the chambers employed in the present study.

a. The chamber was a modification of a structure proposed by Drickamer and Balchan.⁴ The main advantage of this structure was that the plate windows made of hard but brittle materials, such as quartz, sapphire, or diamond, were now made of a material that became plastic at high pressures (single-crystal sodium chloride) and was placed in a narrow long channel. Consequently, the axial pressure was replaced by a hydrostatic pressure and increase in the latter increased the friction of the window material against the channel walls. The adhesion between this material and the walls reduced the pressure from the center of the chamber to the atmospheric value at the periphery. Windows of this kind were capable of withstanding any pressure that could be supported by the walls of the chamber, but cooling caused the outer surface of the window to become covered by a fine network of cracks and partial spallation could be observed. These processes made it practically impossible to carry out optical investigations at low temperatures. Another shortcoming of the Drickamer and Balchan chamber (which applied also to our apparatus) was the depolarization of light transmitted by rock salt layers subjected to different stresses and reflected repeatedly from the channel walls.

b. In the chamber shown in Fig. 1 the windows did not crack even at the lowest temperatures. This was due to the fact that the external layers were compressed so much that they exhibited preferential thermal contraction. Tests carried out over a period of years indicated that a compressed sample could not crack.⁵

c. Tool steels are known to flow or fracture at pressures of 25 kbar. Therefore, higher pressures were reached in our chamber by employing a second stage. The working volume in the first stage was under a pressure of ~ 20 kbar. The working volume of the second stage was under a pressure of ~ 45 kbar (Ref. 6).

2. ANALYSIS OF THE PROCESSES OCCURRING IN THE CASE OF AN ISOLATED $4f$ CONFIGURATION IN A RARE-EARTH ION IN ETHYL SULFATE UNDER COMPRESSION

Rare-earth ethyl sulfates are among the few single crystals whose absorption spectra have been interpreted most reliably.^{7,8} Thin films exhibit only fine lines corresponding to transitions within the $4f$ configuration (Fig. 2). From this point of view the spectrum can be regarded as due to an isolated $4f$ configuration, which is understood to be a configuration of equivalent electrons subject to internal atomic and external crystal fields if the number of states in the spectrum is determined precisely by the number of electrons in this configuration. The energy of the electrostatic interaction between the two f electrons can be described by the expression (Ref. 9, p. 50)

$$\langle LS | 1/r_{1,2} | LS \rangle = \sum_k f_k(l, L) F^k, \quad k=0, 2, 4, 6,$$

where the angular coefficient is

$$f_k(l, L) = (-1)^L \left[(2L+1) (-1)^{(2l+k)/2} \begin{pmatrix} l & k & l \\ 0 & 0 & 0 \end{pmatrix} \right]^2 \left\{ \begin{matrix} l & l & L \\ l & l & k \end{matrix} \right\},$$

and F^0 , F^2 , and F^6 are the radial Slater integrals. In fitting these expressions to the experimental data it is assumed that these integrals are independent parameters.

In the case of the spin-orbit interaction the matrix ele-

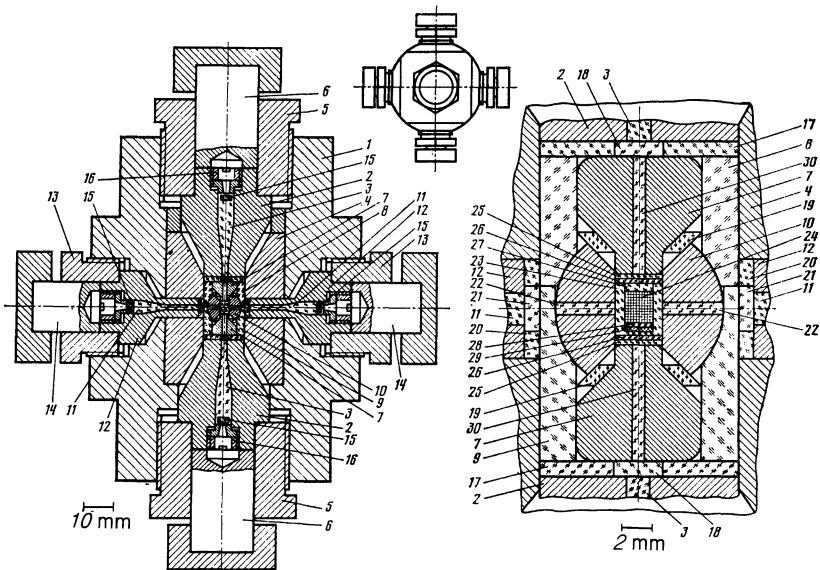


FIG. 1. Six-window low-temperature two-stage chamber: 1) casing; 2), 12) piston; 3), 11), 22), 30) windows made of single-crystal halides; 5), 13), 16) nut; 6), 14) removable piston; 7) piston in the second stage; 8), 9), 23) can made of single-crystal potassium bromide; 10) casing of the second stage ("ball"); 15) piston made of sapphire; 17)–21), 25)–28) spacer made of single-crystal halide; 24) sample; 29) manometer made of ruby.

ment is (Ref. 9, pp. 125, 431)

$$\langle LSJ | H_{so} | L'S'J \rangle = \chi(LS, L'S'J) \zeta_{4f},$$

where

$$\chi(LS, L'S'J)$$

$$= (-1)^{L'+S+J} [l(l+1)(2l+1)]^{1/2} \langle LS || V^{11} || L'S' \rangle \begin{Bmatrix} L & S & J \\ S' & L' & 1 \end{Bmatrix},$$

and ζ_{4f} is a fitting parameter.

A characteristic feature which we encounter on applying the central-field approximation to the configuration of equivalent electrons is that the experimental results yield more numerical data than there are different radial integrals. For example, the f^4 configuration has 47 terms and the energies of all these terms can be described only using four Slater integrals F_k . Naturally, if an allowance is made for the spin-orbit interaction, the situation becomes somewhat more complicated because this interaction splits terms into a large number (107) of separate levels. However, from our point of view, when the amount of experimental data becomes much greater, the theory exhibits still one new parameter which is the spin-orbit interaction constant ζ (Ref. 10). This is true also when calculations include several parameters of the crystal field (it should be noted that the total number of states in an isolated $4f^4$ configuration is 1001).

If the approximation of an isolated $4f$ configuration is valid, the discrepancy between calculations and experiments is less than 1%. This means that the fitting parameters describe satisfactorily the mechanisms postulated in the various theories, i.e., the quantities F_k do indeed govern the Coulomb repulsion between two f electrons and ζ_{4f} represents the spin-orbit interaction. Moreover, it should be noted that the parameters F_k are dependent variables for any type of wave function. Therefore, if we adopt one of the relationships following from this dependence, we can reduce the number of fitting parameters.

We shall assume the following relationships: $F_4/F_2 = 0.15287$ and $F_6/F_2 = 0.01522$ (they follow from the

experimental values of the parameters F_k obtained for the gaseous state of triply charged praseodymium ions).¹¹ The interaction between the $4f^2$ electrons and the external crystal field is described by¹²

$$\langle SLJM | H_{cf} | S'L'J'M' \rangle = \sum_k \sum_q B_k^q (-1)^{J-M} \begin{pmatrix} J & k & J' \\ M & q & M' \end{pmatrix}$$

$$\times (-1)^{S'+L'+J+k} [(2J+1)(2J'+1)]^{1/2} \begin{Bmatrix} J & k & J' \\ L' & S & L \end{Bmatrix}$$

$$\times (-1)^k [(-1)^L + (-1)^{L'}]$$

$$\times [(2L+1)(2L'+1)]^{1/2} \begin{Bmatrix} L & k & L' \\ l & l & l \end{Bmatrix}$$

$$\times (-1)^l (2l+1) \begin{pmatrix} l & k & l \\ 0 & 0 & 0 \end{pmatrix} \delta_{SS'}.$$

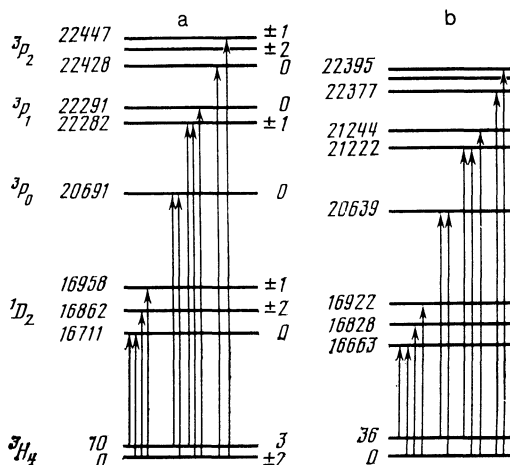


FIG. 2. Part of the scheme of the $4f^2$ configuration of the praseodymium ion in lanthanum ethyl sulfate at zero pressure (a) and 22 kbar (b); Gruber interpretation.⁷ The frequencies of the doublet 3P_1 in Fig. 2a are 21 282 and 21 291 cm^{-1} .

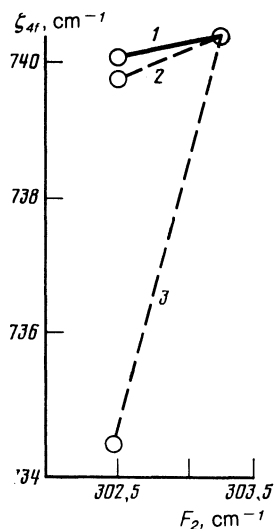


FIG. 3. Change in the spectrum of the $4f^2$ configuration of the praseodymium ion in lanthanum ethyl sulfate compressed by a pressure of 25 kbar; 1) experiment; 2) additional population relationship; 3) Savukinas relationship.¹⁴

It follows from the properties of the $3j$ and $6j$ symbols that $-M + q + M = 0$, $k \leq 2J$, $k \leq 2L$, and $k \leq 2l$.

The parameters of the crystal field are

$$B_k^q = \left(\frac{2k+1}{4\pi} \right)^{1/2} \sum_i \frac{ee_i}{R_i^{k+1}} Y_k^q(\theta_i, \Phi_i),$$

where the indices k and q are related to the use of the Legendre polynomials.

In the subsequent comparison of the experimental and calculated data (see Table II below) it is important that the quantities B_k^q should include R_i , θ_i , and Φ_i , which are the coordinates of the atoms surrounding the central ion.

It has long been known that the parameters of the crystal field calculated *ab initio* do not agree with the experimental results. However, for almost the same time it has also been known that the ratios of the parameters with identical values of k but different values of q are very close to the corresponding experimental ratios. We can therefore assume that the ratios of like parameters obtained experimentally at different pressures, for example at 20 kbar and at the atmospheric pressure, are even closer to the calculated ratios. Therefore, if the approximation of an isolated $4f$ configuration is justified, the spectrum can be described by a point with the coordinates F_2 and ξ_{4f} . Figure 3 shows the change in the spectrum of the $4f^2$ configuration of Pr^{3+} in $\text{La}(\text{C}_2\text{H}_5\text{SO}_4)_3 \cdot 9\text{H}_2\text{O}$ when the sample is compressed from the atmospheric pressure to 25 kbar at helium temperature.

It is clear from this graph that compression reduces the Coulomb repulsion between the f electrons (F_2 changes from $303.3 \pm 0.15 \text{ cm}^{-1}$ to $302.5 \pm 0.2 \text{ cm}^{-1}$), but the spin-orbit interaction is constant within the limits of the experimental error (ξ_{4f} changes from $740.5 \pm 0.4 \text{ cm}^{-1}$ to $740.3 \pm 0.5 \text{ cm}^{-1}$). It follows from theoretical treatments^{13,14} that compression of rare-earth insulators is accompanied by dilatation of wave functions. However, the spin-orbit interaction

constant should then change very greatly: $\Delta\xi/\xi = 3\Delta F_k/F_k$ (Savukinas relationship),¹⁴ which is represented by the dashed line 3 and which is in conflict with the experimental results. We shall therefore assume that compression results in additional population of the $4f$ orbital because of the overlap of the ligand orbitals, i.e., we can expect initial stages of the process

$$4f^2 \rightarrow 4f^3.$$

The Slater integral then changes from 462.62 to 420.04 cm^{-1} and the spin-orbit interaction parameter from 932 to 908 cm^{-1} (Ref. 15), as the wave function is expanded from $\langle r^{-1} \rangle = 0.9245$ to 0.9924 (Ref. 16). This hypothetical process of additional population corresponds to the relationship $3.6\Delta\xi/\xi^{f^2} = \Delta F_2/F_2^{f^2}$ and to the dashed line 2 in Fig. 3.

However, if we compare the data for a "free" praseodymium ion¹¹ ($F_2 = 315.94 \text{ cm}^{-1}$ and $\xi_{4f} = 748.4 \text{ cm}^{-1}$), we find that on reduction of F_2 to 303.3 cm^{-1} the reduction in ξ_{4f} should be 8.37 cm^{-1} , i.e., this quantity should be exactly that observed for lanthanum ethyl sulfate containing neodymium impurities, i.e., 740 cm^{-1} . This corresponds to an additional population representing 0.31 of an electron. It should be stressed that compression to 25 kbar gives rise to no new lines in the spectrum.

Clearly, during the initial stages of the additional population only the antibonding orbitals correspond to the $4f$ electron and the process is accompanied by dilatation of wave functions and weakening of the Coulomb repulsion between electrons, but there are no qualitative changes in the spectrum. However, if these electrons begin to occupy bonding orbitals, the approximation of an isolated f configuration ceases to be valid and the spectrum should exhibit lines representing many-particle interactions. Since in the case of ethyl sulfate this occurs at a pressure of ~ 25 kbar, it is important to know how the crystal structure changes¹⁷ as a result of such compression.

The $\text{Pr}(\text{H}_2\text{O})_9$ complex is shown in Fig. 4 by black dots. The rare-earth ion is at the center. Three water molecules (small triangle) are located above this ion, three are in the same plane (large triangle), and three are below the ion (once again a small triangle). The water molecules are linked by hydrogen bonds to the oxygen ions in the SO_4^{2-} radical. The radical C_2H_5^- is furthest away (Fig. 4 does not

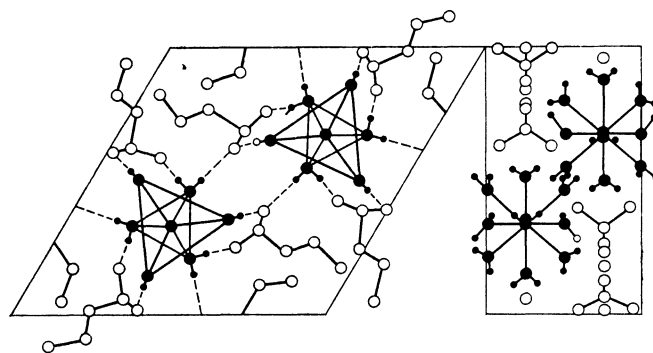


FIG. 4. Structure of praseodymium ethyl sulfate. The $\text{Pr}(\text{H}_2\text{O})_9$ complexes are represented by black dots.

TABLE I. Characteristics of structure groups (radicals).

Radical	Multiplicity of position	Positional symmetry	Symmetry of radical in free state	Ref.
La ³⁺	2c	C _{3h}	—	—
SO ₄ ²⁻	6h	C _s	T _d	[18]
H ₂ O	6h	C _s	C _{2v}	[19]
H ₂ O	12i	C _i	C _{2v}	
C ₂ H ₅ ⁻	6h	C _s	D _{3d} (C ₂ H ₆)	[20]

show the hydrogen ions of this radical).

Table I gives the various characteristics of the structure groups. Table II shows how the distances between the central rare-earth ion and the oxygen in water change in the small and large triangles (R_1 and R_2 , respectively).

These distances have not yet been determined by x-ray structure methods at high pressures. Their values have been estimated from changes in the crystal field parameters²¹ and from the data on the compressibility of the investigated crystal.²² The results calculated allowing for the parameters of the crystal field apply effectively only to the complex formed by the rare-earth ion and nine water molecules, whereas the data allowing for the compressibility are the average values for a macroscopic crystal. Therefore, the agreement between them can be regarded as very good. The transverse compressibility of the complex is almost the same as the compressibility of the whole crystal (17×10^{-4} and 21×10^{-4} kbar⁻¹, respectively). On the other hand, the longitudinal compressibility of the complex is much less than the macroscopic compressibility of the whole crystal (6.6×10^{-4} and 21×10^{-4} kbar⁻¹, respectively). If this is correct, it follows that the water molecules belonging to different complexes located along the Z axis approach each other much more closely. In other words, in reality the Pr-O bond becomes shorter by less than 0.13 Å and the "empty" space between the complexes decreases by more than 0.19 Å.

We shall assume that application of pressures up to 25 kbar reduces the Pr-O₁ distance from 2.47 to 2.38 Å, the Pr-O₂ distance from 2.59 to 2.50 Å, and the O_z-O_z distance from 3.64 to 3.40 Å. This last value is close to the length of

the hydrogen bond in crystals [2.76 Å for an H₂O crystal and 3.33 Å for a Ca(OH)₂ crystal²³]. Therefore, we cannot exclude the possibility that at pressures above 25 kbar the hydrogen bonds in a crystal of ethyl sulfate may become modified forming linear chains: ...Pr...H₂O...H₂O...Pr... (Shishkina and Novak²⁴ were the first to investigate the possibility of a redistribution of a hydrogen bond in a crystal under pressure.)

The populations of the other orbitals of the rare-earth ion can be considered using the EuO₈ complex as an example.²⁵ The calculations are based on the following assumptions.

1. Eight oxygen ions are located on a sphere the radius of which assumes in turn the values 2.8, 2.4, and 2.0 Å.
2. Each of these eight oxygen ions is located at the vertex of a polyhedron.
3. The following polyhedra are considered: cube, dodecahedron, double prism, antiprism, two-cap prism.
4. The ground state of the europium ion has the 4f⁶ configuration.
5. It is assumed that the complex in question has one negative charge.
6. Each europium ion supplies three electrons to the molecular shells: one from the 4f shell and two from the 6s shell.
7. One electron is supplied from a hydrogen atom which is external to the complex.
8. The 2s and 2p shells supply 48 electrons to eight oxygen atoms.
9. The atomic orbitals of oxygen are the radial Slater

TABLE II. Changes of distances between atoms caused by compression of praseodymium ethyl sulfate.

Distance, Å	Deduced from compressibility data ²²		Deduced from changes in quantities B_i^j (Ref. 21)	
	P = 0 kbar	P = 25 kbar	P = 0 kbar	P = 20 kbar
R ₁	2.47	2.34	2.47	2.41
R ₂	2.59 *	2.46	2.65 *	2.56
Pr ₁ -Pr ₂	8.85	8.39	—	—
O _z -O _z	3.64	3.45	—	—
H _z -H _z	2.50	2.37	—	—

*Values of R₂ at 0 kbar differed somewhat in different investigations.

Note. The following notation is used in the above table: R₁ = Pr-O₁ is the distance between the central ion and an oxygen ion in the small triangle; R₂ = Pr-O₂ is the distance between the central ion and an oxygen ion in the large triangle; Pr₁-Pr₂ is the distance between the centers of two complexes in one unit cell; O_z-O_z is the distance between the oxygen ions in the lower small triangle of the complex in one unit cell and the upper small triangle of the complex in the second unit cell located along the Z axis; H_z-H_z; is the same but for the hydrogen ions.

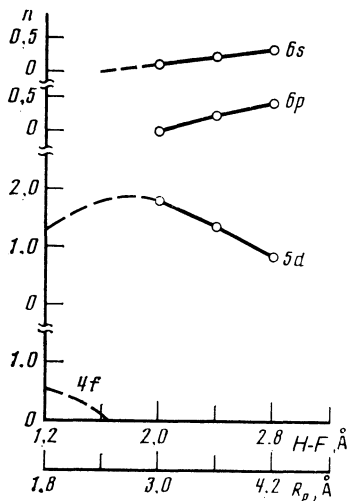


FIG. 5. Postulated redistribution of the electron populations of the atomic orbitals in the process of compression of a rare-earth-oxygen complex.

functions and the orbitals of the central atom are described by analytic expressions proposed and programmed by A. K. Kantseriyavichus.²⁶

The data for an antiprism are presented in Fig. 5. The dashed curves represent the postulated process of additional population of the $4f$ orbital, which should begin when the rare-earth ion approaches an oxygen ion to a distance of ~ 2.4 Å. Since the radial integrals obtained allowing for the Hartree-Fock functions are ~ 1.5 times greater than the corresponding quantities found experimentally, it is assumed that the real wave functions are correspondingly dilated. In going over from the distances obtained using the Hartree-Fock functions to the real distances, we shall also use the coefficient 1.5 and this is reflected by the lower scale of the abscissa in Fig. 5. It is clear from this figure that when the distance between the rare earth ion and an oxygen ion is greater than the real distance in a crystal (~ 2.4 Å), the chemical binding should be due to the $6s$, $6p$, and $5d$ electrons. However, for a distance of ~ 3.0 Å the binding is almost entirely due to the $5d$ electrons. In view of their multiple dumbbell nature (according to I. B. Bersuker²⁷), the $5d$ orbitals displace the $6p$ orbitals. In other words, the electrons from the $6p$ orbital fill the $5d$ orbital. We can assume that on further reduction in the distance even the $5d$ orbital begins to lose electrons to the $4f$ orbital.

3. ANALYSIS OF THE PROCESSES RESULTING IN LOSS OF ISOLATION BY THE $4f$ CONFIGURATION OF RARE-EARTH IONS IN ETHYL SULFATES

Naturally, the molecular orbital methods are only very rough. Therefore, Fig. 5 should be regarded only as a tentative model. However, we can consider what should happen if this model describes the reality correctly.

Jahn and Teller²⁸ said that the degeneracy of the ground state in rare-earth salts is due to the fact that the f electrons do not participate in the chemical binding, i.e., the symmetry does not decrease not because there is no corresponding vibration but because there is practically no electron-vibration

interaction. However, as soon as the f electrons become responsible for the chemical binding, this interaction appears and the degeneracy should be lifted. The spectrum of the praseodymium ion itself should exhibit vibronic states because "in the presence of electron degeneracy the adiabatic approximation is invalid ... the nuclear and electronic motion is completely mixed and the states of the system become electron-nuclear (vibronic)" (Ref. 27, p. 201). [Naturally, if a crystal contains only 1% of the Pr^{3+} impurity, then this impurity should not affect the energy state of the crystal. From the point of view of collective interaction we can expect a major difference between the behavior of LaES (1% Pr^{3+}), PrES (i.e., 100% Pr^{3+}), and LaES (10% Nd^{3+}) crystals for which the Kramers degeneracy of the ground state does not result in the Jahn-Teller effect, but this is contrary to the experimental observations.]

Since the model of Fig. 5 postulates the participation of the f electrons in the chemical binding only from a certain distance, it follows that the $\text{Pr}(\text{H}_2\text{O})_9$ complex should contain bonds of different kinds between the central rare-earth ion and the ligands. For example, the $\text{Pr}-\text{O}_1$ bond (with an oxygen in the small triangle) which has the length of 2.38 Å at 25 kbar should be due to the f electrons and should be manifested in the spectrum by vibronic states, whereas the $\text{Pr}-\text{O}_2$ bond (with an oxygen in the large triangle) has a length in excess of 2.50 Å and it should be due to the d electrons but should not appear in the spectrum associated with the $4f$ configuration. However, we can expect that at pressures above 70 kbar the spectrum will include also the vibronic states associated with the $\text{Pr}-\text{O}_2$ chemical bond.

It is worth making another comment. It is clear from Fig. 4 that there is a system of chemical bonds between the rare-earth ions in a crystal cell. At atmospheric pressures this results in some interaction between the d configurations of the rare-earth ions because both the $\text{Pr}-\text{O}_1$ and the $\text{Pr}-\text{O}_2$ bonds are due to the d electrons. In the investigated range of pressures (25–50 kbar) the f configuration of one ion (the $\text{Pr}-\text{O}_1$ bond is governed now by the f electrons) interacts with the d configuration of another ion (the $\text{Pr}-\text{O}_2$ bond is still governed by the d electrons). Finally, at pressures above 70 kbar the interaction between the f configurations of both ions should be manifest and this should result in magnetic ordering at some temperature.

It has been assumed so far that the spectrum of rare-earth ethyl sulfates can be interpreted reliably and, therefore, the theoretical parameters describe it satisfactorily.²⁹ However, the changes which occur in the spectrum of lanthanum ethyl sulfate containing praseodymium or neodymium as an impurity on attainment of the critical distance (2.38 Å) between the rare-earth ion and one oxygen ion or a group of such ions do not fit the approximation of an isolated $4f^2$ configuration so that it is necessary to turn back to the initial information presented by the "external" form of the spectrum.

Figure 6 shows the spectrum of 1% Pr in LaES in the region of the ${}^3H_4(\pm 2) \rightarrow {}^3P_0(0)$ transition, i.e., in the region where one line is exhibited by an isolated $4f^2$ configuration at 4 K. At liquid nitrogen temperature a certain position of the sample can ensure that a line associated with the first

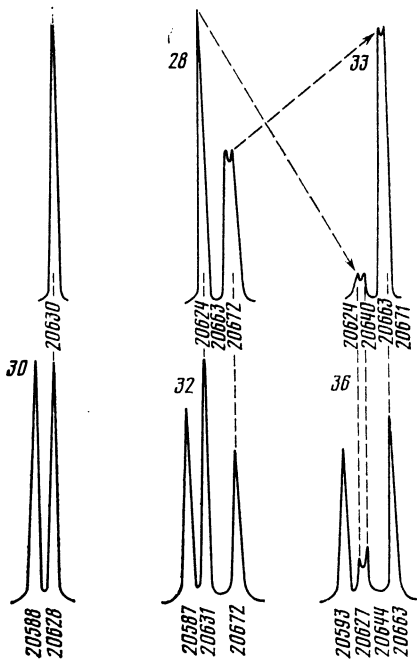


FIG. 6. Absorption spectrum of a sample with 1% praseodymium in lanthanum ethyl sulfate in the region of the ${}^3H_4(\pm 2) \rightarrow {}^3P_0(0)$ transition in the case of light propagating parallel (upper part of the figure) and perpendicular (lower part of the figure) to the crystal axis. Pressures from 25 to 36 kbar (given by numbers at top of the spectra), $T = 78$ K, frequency in reciprocal centimeters.

excited level is also observed.

Figure 7 shows the spectrum of the sample obtained also for $l \parallel Z$, but in the region of the ${}^3H_4(\pm 2) \rightarrow {}^1D_2$ transition. The dashed lines demonstrate a single spectral line due to the ${}^3H_4(\pm 2) \rightarrow {}^1D_2(0)$ transition and the subsequent splitting of this spectral line. Figure 8 shows the spectrum of a sample of LaEs with 10% Nd in the region of the ${}^4I_{9/2}(\pm 5/2) \rightarrow {}^2P_{1/2}(\pm 1/2)$ transition, i.e., in the region where one line should be observed for an isolated $4f^3$ configuration. The pattern is the same in all these cases. When a certain pressure is attained, the purely electronic and reliably interpreted spectrum disappears (or its intensity falls drastically), and instead there is a spectrum which we shall

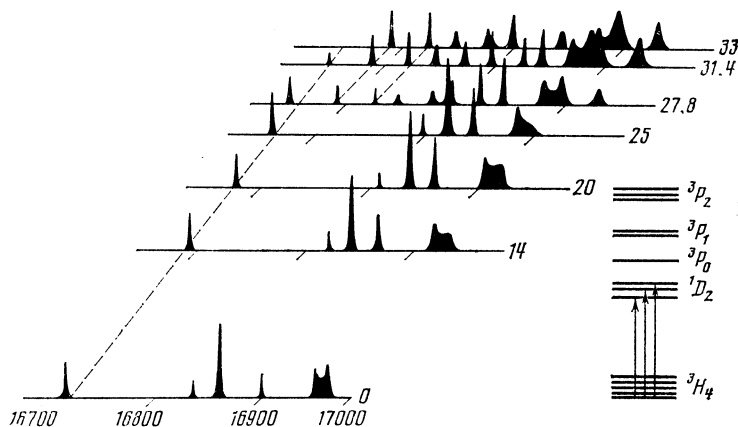


FIG. 7. Absorption spectrum of a sample with 1% praseodymium in lanthanum ethyl sulfate in the region of the ${}^3H_4(\pm 2) \rightarrow {}^1D_2$ transition for light propagating parallel to the crystal axis. Pressures from 0 to 33 kbar (numbers alongside the axes), $T = 78$ K, frequency in reciprocal centimeters.

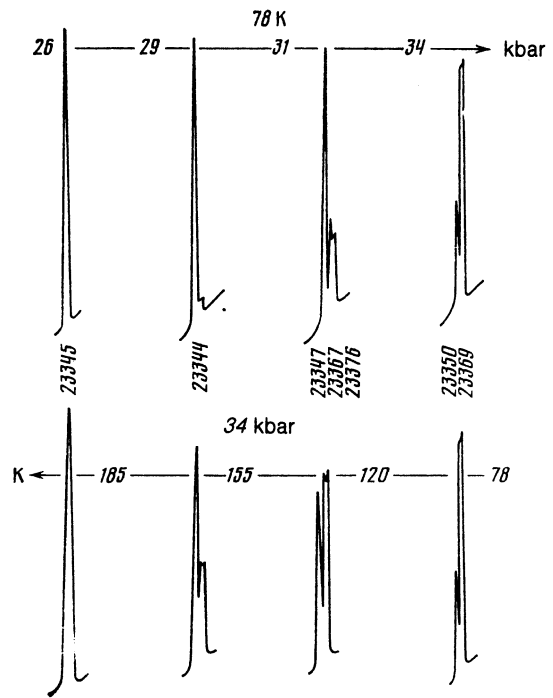


FIG. 8. Absorption spectrum of a sample with 10% neodymium in lanthanum ethyl sulfate in the region of the ${}^4I_{9/2}(\pm 5/2) \rightarrow {}^2P_{1/2}(\pm 1/2)$ transition. Pressure from 26 to 34 kbar (numbers at the top of the spectra), temperature from 78 to 185 K, frequency in reciprocal centimeters.

call vibronic and which exhibits a split line (Table III).

When a sample compressed to 40 kbar is heated, the vibronic state is destroyed at $T = 160$ K and we once again observe the purely electronic spectrum. (It should be noted that the vibronic state of a sample compressed to 50 kbar is not destroyed by heating up to 180 K. Clearly, the distance $Pr-O_1$ decreases so much that the thermal vibrations cannot increase it to $R > 2.38$ Å.)

Table IV gives the results obtained by recording the Raman scattering spectrum of an LaES single crystal at various pressures, as well as the results of an analysis of this spectrum.^{30,31}

These results can be summarized briefly as follows.

TABLE III. Splitting of vibronic line and gap between this line and purely electronic line.

Region	Splitting, cm^{-1}	Gap, cm^{-1}
$4f^2 : {}^3H_4(\pm 2) \rightarrow {}^1D_2(0)$	35 ± 3	56 ± 3
$4f^2 : {}^3H_4(\pm 2) \rightarrow {}^3P_0(0)$	8 ± 3	44 ± 3
$4f^2 : {}^3H_4(3) \rightarrow {}^3P_1(\pm 1)$	16 ± 3	42 ± 3
$4f^3 : {}^4I_{3/2}(\pm 5/2) \rightarrow {}^2P_{1/2}(\pm 1/2)$	9 ± 3	25 ± 3

1. A series of low-frequency lines is shifted toward lower frequencies at pressures up to 27 kbar, but it disappears at 34 kbar, which is attributed to the formation of a vibronic state, or the intensity of these lines decreases drastically. (According to Ref. 32, the low-frequency lines exhibit an anomalous temperature dependence.)

2. The doubly degenerate lines become split explicitly or are smeared out (in this case the symbol \sim is used in front of the value in Table IV).

3. The obviously nondegenerate line at 1073 cm^{-1} remains sharp and strong, indicating that two centers, cell doubling, or similar effects do not occur.

One should mention also alternative explanations of the observed behavior.

1. When the phase transition takes place, the symmetry is reduced, the purely electronic line is shifted, and the ground state is split. Attempts to account for the splitting of the spectral absorption lines by lowering of the symmetry within the framework of the approximation of an isolated $4f$

configuration meet directly with many contradictions. Bearing in mind only the observations reported above, these contradictions are as follows. Judging by the transitions to ${}^1D_2(0)$, the splitting of the ground state should be $\sim 35 \text{ cm}^{-1}$, whereas judging by the transition to 3P_0 , it should be $\sim 8 \text{ cm}^{-1}$. Lowering of the symmetry does not lift the Kramers degeneracy of the levels of the $4f^3$ configuration.

2. We may assume that two centers are formed and that the split line represents the same ${}^3H_4(\pm 2) \rightarrow {}^3P_0(0)$ transition, but having somewhat different energies. This is in conflict with the absence of the same splitting in the case of the nondegenerate Raman scattering lines.

3. It is possible that "new" lines represent the spectrum of pair centers, i.e., the result of the interaction of the nearest rare-earth ions (this would seem particularly likely because pair centers have been observed in rare-earth ethyl sulfates although by methods more sensitive than optical spectroscopy).^{33,34} However, in this case the relative intensities of the "new" lines should differ strongly in the case of 1% Pr in

TABLE IV. Raman spectra of lanthanum ethyl sulfate at 78 K.

Ag	P = 0 kbar		P = 17 kbar	P = 34 kbar	Ref.
	E_{2g}	E_{1g}			
—	—	36,5	—	—	LaO ₉
—	—	67	41 *	—	
—	—	92	69	—	
—	—	114	—	—	
—	128	130	—	—	
166	166	—	152	—	
—	—	197	189	—	O...H-O
—	221	—	—	—	
—	—	238	—	—	
263	263	263	263	—	
—	—	313	320	~ 316	SO ₄ ²⁻
346	—	—	—	—	
—	353	—	357	357	C ₂ H ₅ ⁻
363	—	—	361	373	
—	423	421	—	—	SO ₄ ²⁻
427	—	433	433	~ 441	
489	485	—	494	—	
576	—	576	581	~ 573	C ₂ H ₅ ⁻
—	616	—	617	—	
809	809	(809)	828	$824/830$	C ₂ H ₅ ⁻
—	928	—	—	—	
936	—	—	947	947	C ₂ H ₅ ⁻
1012	1012	—	1027	$1019/1027$	
1073	—	—	1091	1087	SO ₄ ²⁻
1113	1111	—	1122	1122	
—	—	1202	1200	1200	C ₂ H ₅ ⁻
—	—	1292	1300	$1300/1307$	
1394	1397	—	$1406/1408$	$1402/1415$	C ₂ H ₅ ⁻
1448	1448	1448	1450	$1439/1453$	
1467	1476	—	1475	1471	

*Results obtained at 27 kbar.

TABLE V. Spectrum of cesium dysprosium molybdate at 1300 cm^{-1} obtained under different thermodynamic conditions.

$P = 0\text{ kbar}$		$P = 8\text{ kbar}$		$P = 13.6\text{ kbar}$	
$T = 4.2\text{ K}$	$T = 77\text{ K}$	$T = 4.2\text{ K}$	$T = 77\text{ K}$	$T = 4.2\text{ K}$	$T = 77\text{ K}$
A	—	$13334/13327$	13 320	$13329/13321$	—
B	13 244	$13282/13255$	13 245	$13261/13253$	13 250
C	13 202	—	13 205	$13214/13202$	13 203
D	13 158	—	13 158	—	13 152 13 115

lanthanum ethyl sulfate and of pure praseodymium ethyl sulfate, which is not found experimentally. Moreover, we checked this hypothesis by growing a mixed crystal containing Pr and Nd impurities in lanthanum ethyl sulfate. In the case of formation of pairs, in addition to the spectrum of Pr-Pr and Nd-Nd pairs there should be also a spectrum of Pr-Nd pairs. However, the spectrum of a mixed crystal was fully additive at high pressures.

It thus follows that the hypothesis of a vibronic state is so far the only possible explanation, but it needs further confirmation. This confirmation should be provided, in particular, by the appearance of a second vibronic line in the spectrum of praseodymium ethyl sulfate on reductions of the Pr-O₂ distance to 2.38 Å and naturally by observations of a similar pattern in the case of other samples.

4. ANALYSIS OF THE PROCESSES OCCURRING IN CESIUM DYSPROSIUM MOLYBDATE DUE TO CHANGES IN THERMODYNAMIC CONDITIONS

The crystal structure not of CsDy(MoO₄)₂ but of CsPr(MoO₄)₂ has been described in detail.³⁵ The praseodymium ion is inside a figure with eight oxygens at the vertices in which four distances at room temperature and atmospheric pressure are Pr-O₁ = 2.38 Å and the other four are Pr-O₂ = 2.54 Å. Therefore, already at atmospheric pressure the *f* electrons should participate in the chemical binding between the praseodymium ion and four oxygen atoms, and

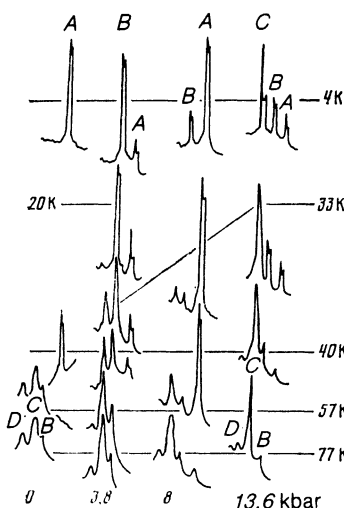


FIG. 9. Spectrum of cesium dysprosium molybdate in the region of $13\ 100\text{--}13\ 400\text{ cm}^{-1}$. Pressure from 0 to 14 kbar, temperature from 4.2 to 78 K, frequency in reciprocal centimeters.

the spectrum associated with the 4*f* configuration should be manifested by the appearance of a vibronic state.

At a constant atmospheric pressure and on increase in the temperature from 4 to 40 K the CsDy(MoO₄)₂ spectrum recorded in the region of 1300 cm^{-1} is characterized by one split ($\sim 7\text{ cm}^{-1}$) line *A*, whereas at higher temperatures three diffuse lines *B*, *C*, and *D* are observed (Fig. 9, Table V). The nature of changes in the temperature dependence of the specific heat shows that at atmospheric pressure and 42 K a first-order phase transition takes place.^{36,37}

At a constant helium temperature an increase in pressure to 3.8 kbar also alters qualitatively the spectrum. Before the split line *A*, there is also a split ($\sim 8\text{ cm}^{-1}$) line *B* with a gap of $\sim 74\text{ cm}^{-1}$ between *A* and *B*. Once again the line *A* disappears on heating above 40 K, but the line *B* simply loses its high-frequency component. Moreover, a line *C* appears well before 40 K and between 20 and 40 K it coexists with the line *A* (the intensity of the line *A* falls and that of the *C* rises). A line *D* also coexists with the line *A*, although this happens in a narrower temperature interval. Judging by the spectral data, at 3.8 kbar the phase transition occurs in certain stages, one of which begins at a lower temperature than the thermal transition and the other is completed at a higher temperature than this transition. A constant helium temperature and increase in pressure to 13.6 kbar once again alters the spectrum qualitatively. In addition to the lines *A* and *B*, the split ($\sim 12\text{ cm}^{-1}$) line *C* is now observed. However, heating to just 33 K suppresses the splitting of this line and at 40 K the line *D* is observed.

Within the hypothesis put forward above, which states that the vibronic line corresponds to the chemical binding of the rare-earth ion with a specific oxygen ion (when the critical distance between them becomes 2.38 Å), and also bearing in mind that these lines appear and disappear as a result

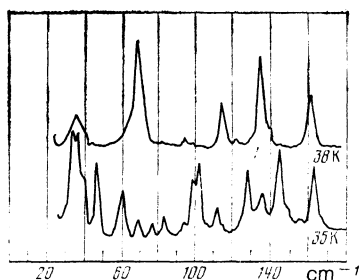


FIG. 10. Raman scattering spectrum of cesium dysprosium molybdate at low frequencies recorded at atmospheric pressure at temperatures close to the phase transition (according to Ref. 39), between 35 and 38 K.

of very slight changes in the volume (thermal expansion or application of very low pressures), we have to assume that the observed behavior represents a gradual increase of participation of the f electrons in four Dy–O₁ bonds. At the atmospheric pressure and helium temperature is only one bond due to the f electrons and the bond length is $R < 2.39 \text{ \AA}$, whereas the other three are due to the d electrons and the bond length is $R > 2.38 \text{ \AA}$. This would suggest that the high-temperature phase should have a smaller volume than the low-temperature phase. Direct x-ray diffraction investigations also confirm that "on transition to the high-temperature phase the lattice becomes compressed" (Ref. 38).

It has been suggested above that the formation of a vibronic state is accompanied by the disappearance of purely electronic lines from the spectrum as well as of the lines of the vibrations mixed with this vibronic state. Figure 10, based on the data of Ref. 39, shows that the frequencies $\sim 60 \text{ cm}^{-1}$, $\sim 105 \text{ cm}^{-1}$, and $\sim 145 \text{ cm}^{-1}$ disappear on heating above the thermal phase transition.

We can therefore assume that the purely electronic line should have the energy $E \sim 13\,100 \text{ cm}^{-1}$ ($13\,158 - 60 = 13\,098$; $13\,202 - 105 = 13\,097$; $13\,244 - 145 = 13\,099$); conversely, heating should give rise to a frequency corresponding to the "breakup" of the $13\,339/13\,331$ vibronic line into a purely electronic line at $\sim 13\,100 \text{ cm}^{-1}$ and a vibrational one $\nu = 235 \text{ cm}^{-1}$.

In fact, according to Ref. 39, such a strong line is observed in the infrared spectrum at room temperature (no information is given on this part of the spectrum below the phase transition point). Clearly, the hypothesis of the formation and breakup of vibronic states still requires careful theoretical and experimental study. On the one hand if it is correct, then in the region of $13\,000 \text{ cm}^{-1}$ only one purely electronic transition takes place, which requires an explanation from the point of view of its treatment as the ${}^6H_{15/2} \rightarrow {}^6F_{3/2}$ transition.^{40–42}

The author is grateful to A. I. Zvyagin and L. F. Chernysh for supplying molybdate and ethyl sulfate crystals, and to A. I. Kas'yanov and V. P. Kondratenko for their help in the experiments.

¹V. A. Voloshin, L. A. Ivchenko, and V. I. Rublinetskiĭ, 6-ĭ Vsesoyuznyĭ simpozium po spektroskopii kristallov, aktivirovannykh ionami redkozemel'nykh i perekhodnykh metallov. Tezisy dokladov (Abstracts of Papers presented at Sixth All-Union Symposium on Spectroscopy of Crystals Activated with Ions of Rare-Earth and Transition Metals), Nauka, M., 1979, p. 77.

²V. A. Voloshin and L. A. Ivchenko, Pis'ma Zh. Eksp. Teor. Fiz. **32**, 111 (1980) [JETP Lett. **32**, 100 (1980)].

³I. V. Skorobogatova, E. M. Savchenko, V. A. Voloshin, and A. I. Zvyagin, 7-ĭ Vsesoyuznyĭ simposium po spektroskopii kristallov, aktivirovannykh ionami redkozemel'nykh i perekhodnykh metallov. Tezisy dokladov (Abstracts of Papers presented at Seventh All-Union Symposium on Spectroscopy of Crystals Activated with Ions of Rare-Earth and Transition Metals), Nauka, Leningrad, 1982, p. 72.

⁴H. G. Drickamer and A. S. Balchan, in: Modern Very High Pressure Techniques (ed. by R. H. Wentorf Jr.), Butterworths, London (1962) [Russ. Transl., Mir, M., 1964, p. 51].

⁵V. A. Voloshin and A. I. Kas'yanov, Prib. Tekh. Eksp. No. 1, 203 (1980).

⁶V. A. Voloshin and A. I. Kas'yanov, Prib. Tekh. Eksp. No. 5, 170 (1982).

⁷J. B. Gruber, J. Chem. Phys. **38**, 946 (1963).

⁸J. B. Gruber, and R. A. Satten, J. Chem. Phys. **39**, 1455 (1963).

⁹A. P. Yutsis and A. Yu. Savukinas, Matematicheskie osnovy teorii atoma (Mathematical Basis of the Theory of the Atom), Mintis, Vilnius, 1973, p. 480.

¹⁰B. R. Judd, *Operator Techniques in Atomic Spectroscopy*, McGraw-Hill, New York, 1963 (Russ. Transl., Mir, M., 1970).

¹¹J. Sugar, Phys. Rev. Lett. **14**, 731 (1965).

¹²D. A. Wensky and W. G. Moulton, J. Chem. Phys. **53**, 423 (1970).

¹³C. K. Jørgensen, K. Dan. Vidensk. Selsk. Mat.-Fys. Medd. **30**, No. 22 (1956).

¹⁴A. Yu. Savukinas, K. P. Ėriksonas, and N. A. Kulagin, Programma i tezisy V Mezhdunarodnoĭ konferentsii po fizike i tekhnike vysokikh davlenii (Program and Abstracts of Papers presented at Fifth Intern. Conf. on Physics and Technology of High Pressures), Nauka, M., 1975, p. 84.

¹⁵S. D. Shadzhuyvene, R. T. Surgailene, P. V. Ripskite, P. O. Bogdanovichyus, and R. I. Karaziya, Litov. Fiz. Sb. **10**, 873 (1970).

¹⁶K. M. S. Saxena and G. Malli, Technical Report TR-1970-01, Department of Chemistry, Simon Fraser University, Burnaby, B.C., Canada, 1970.

¹⁷J. Albertsson and I. Elding, Acta Crystallogr. Sect. B **33**, 1460 (1977).

¹⁸H. Poulet and J. P. Mathieu, *Vibrational Spectra and Symmetry of Crystals*, Gordon and Breach, Paris, 1970 (Russ. Transl., Mir, M., 1973, p. 437).

¹⁹G. R. Wilkinson, in: Applications of Raman Spectra (Russ. Transl., ed. by K. I. Petrov), Mir, M., 1977, p. 586.

²⁰H. P. Geserich, K. H. Hellwege, and G. Z. Schaack, Z. Naturforsch. Teil A **20**, 289 (1965).

²¹V. A. Voloshin, L. A. Ivchenko, I. M. Krygin, G. N. Neĭlo, A. D. Prokhorov, and V. I. Rublinetskiĭ, Fiz. Tekh. Vys. Davlenii No. 8, 25 (1982).

²²S. N. Lukin, G. N. Neĭlo, A. D. Prokhorov, and G. A. Tsintsadze, Fiz. Tverd. Tela (Leningrad) **23**, 3070 (1981) [Sov. Phys. Solid State **23**, 1789 (1981)].

²³G. C. Pimentel and A. L. McClellan, *The Hydrogen Bond*, Freeman, San Francisco, 1960 (Russ. Transl., Mir, M., 1964, p. 462).

²⁴N. I. Shishkin and I. I. Novak, Zh. Tekh. Fiz. **23**, 1485 (1953).

²⁵Yu. Narushis, V. Lazauskas, and V. Voloshin, Litov. Fiz. Sb. **21**, 3 (1981).

²⁶A. K. Kantseryavichus, Programma dlya vychisleniya analiticheskikh radial'nykh orbital'ei, GFAP No. 000518 (Program for Calculation of Analytic Radial Orbitals, GFAP No. 000518), Vilnius, 1974.

²⁷I. B. Bersuker, Ėlektronnoe stroenie i svoĭstva koordinatsionnykh soedinenii (Electronic Structure and Properties of Coordination Compounds), Khimiya, Leningrad, 1976, p. 348.

²⁸H. A. Jahn and E. Teller, Proc. R. Soc. London Ser. A **161**, 220 (1937).

²⁹B. G. Wybourne, *Spectroscopic Properties of Rare Earths*, Interscience, New York, 1965.

³⁰V. A. Voloshin, A. K. Kupchikov, and Yu. G. Pashkevich, Terzisy dokladov. Kraevaya konferentsiya po KRS (Abstracts of Papers presented at Regional Conference on Raman Spectroscopy), Krasnoyarsk, 1983, p. 136.

³¹V. A. Voloshin, A. K. Kupchikov, and Yu. G. Pashkevich, V sb.: Nelineĭnaya optika i spektroskopiya molekulyarnykh sred (in: Nonlinear Optics and Spectroscopy of Molecular Media), Izd. AN SSSR, Krasnoyarsk, 1984, p. 88.

³²G. Schaack and J. A. Koningstein, Can. J. Chem. **51**, 1023 (1973).

³³J. M. Baker, J. Phys. C **4**, 1631 (1971).

³⁴I. M. Krygin and A. D. Prokhorov, Zh. Eksp. Teor. Fiz. **86**, 590 (1984) [Sov. Phys. JETP **59**, 344 (1984)].

³⁵R. F. Klevtsova, V. A. Vinokurov, and P. V. Klevtsov, Kristallografiya **17**, 284 (1972) [Sov. Phys. Crystallogr. **17**, 240 (1972)].

³⁶E. E. Anders, A. I. Zvyagin, and L. S. Shestachenko, Fiz. Nizk. Temp. **6**, 1356 (1980) [Sov. J. Low Temp. Phys. **6**, 661 (1980)].

³⁷E. E. Anders, A. I. Zvyagin, S. V. Startsev, and L. S. Shestachenko, Fiz. Nizk. Temp. **9**, 1218 (1983) [Sov. J. Low Temp. Phys. **9**, 629 (1983)].

³⁸S. D. El'chaninova, A. I. Zvyagin, and Z. A. Kazeĭ, Fiz. Nizk. Temp. **8**, 303 (1982) [Sov. J. Low Temp. Phys. **8**, 152 (1982)].

³⁹N. M. Nesterenko, V. I. Fomin, V. I. Kut'ko, and A. I. Zvyagin, Issledovaniya strukturnogo fazovogo perekhoda CsDy(MoO₄)₂ po fononnykh spektram [Investgations of a Structural Phase Transition in CsDy(MoO₄)₂ on the Basis of Phonon Spectra], Preprint No. 26-82, Physicotechnical Institute of Low Temperatures, Kharkov, p. 36.

⁴⁰B. G. Wybourne, J. Chem. Phys. **36**, 2301 (1962).

⁴¹M. Veyssie and B. Dreyfus, J. Phys. Chem. Solids **28**, 499 (1967).

⁴²G. H. Dieke, *Spectra and Energy Levels of Rare Earth Ions in Crystals*, Interscience, New York, 1968, p. 401.

Translated by A. Tybulewicz